Promoting the Reduction Reactivity of Ilmenite by Introducing Foreign Ions in Chemical Looping Combustion

ARTICLE *in* INDUSTRIAL & ENGINEERING CHEMISTRY RESEARCH · APRIL 2013

Impact Factor: 2.59 · DOI: 10.1021/ie400237p

3 AUTHORS, INCLUDING:

Ningsheng Cai
Tsinghua University
138 PUBLICATIONS **1,797** CITATIONS

SEE PROFILE

I&EC research
Industrial & Engineering Chemistry Research

Article

pubs.acs.org/IECR

Promoting the Reduction Reactivity of Ilmenite by Introducing Foreign Ions in Chemical Looping Combustion

Jinhua Bao, Zhenshan Li,* and Ningsheng Cai

Key Laboratory for Thermal Science and Power Engineering of Ministry of Education, Beijing Municipal Key Laboratory for CO_2 Utilization & Reduction, Department of Thermal Engineering, Tsinghua University, Beijing 100084, China

ABSTRACT: A new kind of ilmenite oxygen carrier was prepared by impregnating the raw ilmenite particles with K_2CO_3, Na_2CO_3, or $Ca(NO_3)_2$. The cyclic reduction reactivity of the new oxygen carrier was investigated in a fluidized bed reactor. It has been found that the addition of foreign ions can significantly promote the reduction reactivity of ilmenite. The effect of foreign ions on enhancing the reduction reactivity of ilmenite is in the sequence of $K^+ > Na^+ > Ca^{2+}$. The effect of the loading amount of K^+ on increasing the ilmenite reactivity is in the sequence of 15 wt % K^+ > 10 wt % K^+ > 5 wt % K^+. The reduction reactivity of the ilmenite impregnated with 15 wt % K^+ can be improved ~8 times faster than that of the activated raw ilmenite. This reactivity reaches up to the same level of the synthetic Ni-based carrier. The modified ilmenite obtains a porous structure caused by the migration of K or Na ions. One possible explanation for the reactivity enhancement of ilmenite with the addition of foreign ions, especially K^+ and Na^+, is the migration of K^+ or Na^+. Another explanation may be the active principle of the alkali-rich phase formed between the foreign ions and titanium iron oxides, that is, $K_{1.46}Ti_{7.2}Fe_{0.8}O_{16}$ or $Na_2Fe_2Ti_6O_{16}$. This study proves that the reduction reactivity of the natural ilmenite can be promoted significantly by impregnating ilmenite with K^+.

1. INTRODUCTION

Chemical looping combustion (CLC), introduced by Richter and Knoche,[1] has emerged as an attractive option for separating the greenhouse gas CO_2.[2,3] This technique is based on the use of an oxygen carrier (usually a transition metal oxide) that transports the oxygen required for combustion from the air to the fuel, avoiding direct contact between fuel and air. The CLC process, as represented in Figure 1, consists of two interconnected reactors, a fuel reactor and an air reactor. In the fuel reactor, the oxygen carrier is reduced by the fuel, and the reduced oxygen carrier is oxidized back to its original state in the air reactor. The exit gas from the fuel reactor contains CO_2 and H_2O, which is not diluted by N_2 from the air. By condensing the steam, high-purity CO_2 can be obtained, without energy penalty for separation. After the development of the CLC concept in lab-scale testing facilities, such as the thermogravimetric analyzer (TGA), the fixed bed, and the batch fluidized bed, a CLC system with two interconnected fluidized bed reactors was proposed by Lyngfelt et al.[4] in 2001, and successfully demonstrated for gaseous fuels in 2003.[5] The concept of CLC is now being demonstrated in large pilot scale, such as the 100 kWth plant for solid fuel in Chalmers,[6] the 120 kWth plant for gas fuels in Vienna,[7] the 1 MWth plant for solid fuel in Damstandt,[8] the 3 MWth Plant for solid fuel by Alstom in Windsor,[9] and the 10 MWth plant for gas fuel to be built for commercial operation in Canada.[10] Therefore, CLC is a promising technology for CO_2 capture and electricity or heat production.

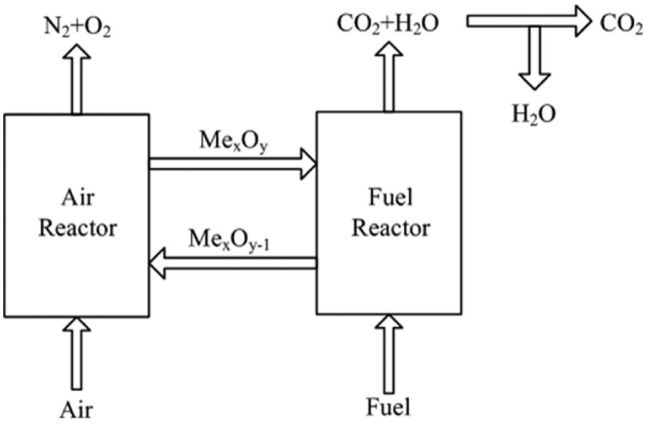

Figure 1. Schematic diagram of a chemical looping combustion system.

In the practical application of CLC, the oxygen carrier is used in many reduction−oxidation cycles. Therefore, the suitable carrier should have a low cost, no toxins, and high reactivity. The oxygen transporting capacity and selectivity toward CO_2 and H_2O is important, as well as the resistance to agglomeration and attrition. Many kinds of oxygen carriers have been studied and can be summarized briefly as follows: (i) Different metal oxides based on Fe, Cu, Ni, Mn, and Co have been proposed and tested as suitable oxygen carriers. (ii) Many inert supports, including Al_2O_3, SiO_2, MgO, TiO_2, ZrO_2, cement,[11] sepiolite, etc., have been tested for synthetic oxygen carriers. Some of these supports can resist high temperature sintering of metal or oxide grain, improve cyclic reactivity, and resist agglomeration and attrition. (iii) Various preparation methods, such as mechanical mixing, wet impregnation, coprecipitation, freeze-granulated, spray-dry, sol−gel, dissolution, etc., were tested to incorporate inert support particles into

Received: January 22, 2013
Revised: April 14, 2013
Accepted: April 15, 2013
Published: April 15, 2013

oxygen carrier particles. Recent reviews have extensively summarized the published works.[12,13] In general, synthetic carriers have been proven to be feasible for CLC with gaseous fuels.[14−16] Since ash exists in the direct use of solid fuels, removal of the ash from the reactors is required in order to avoid ash accumulation. In this case, low-cost oxygen carriers, such as natural minerals, are preferred in consideration of their partial loss together with the fuel ash removal from the reactor. Therefore, the search for and testing of cheap oxygen carriers is necessary and meaningful for the development of CLC with solid fuels. From this point, natural Fe-, Mn-, and Cu-based ores[17−23] and industrial residues[23,24] have been considered as attractive options for solid fuel CLC because of their low cost, nontoxicity, and abundance. Among all these oxygen carriers, ilmenite, a natural mineral composed of $FeTiO_3$, is a low cost, attractive material and has been tested extensively. Table 1 gives some of the most important work done with ilmenite.

Table 1. Some of the Most Important Work Done with Ilmenite As the Oxygen Carrier in CLC

author	location	apparatus	fuel	year[a]	reference
Lab Scale Test Facility: TGA, Fixed Bed, and Batch Fluidized Bed					
Adanez et al.	CSIC[b]	TGA	H_2, CO, CH_4	2010	25
Abad et al.	CSIC	TGA	H_2, CO, CH_4	2011	26
Leion et al.	Chalmers	FB	CO, H_2	2008	27
Leion et al.	Chalmers	FB	coal	2008	28
Azis et al.	Chalmers	FB	CO, H_2	2010	29
Cuadrat et al.	CSIC	FB	H_2, CO, CH_4	2012	30
Schwebel et al.	Siegen	FB	CO	2012	31
Interconnected Fluidized Bed Reactors					
Cuadrat et al.	CSIC	500 Wth	coal	2011	32
Berguerand et al.	Chalmers	10 kWth	coal	2008	33
Berguerand et al.	Chalmers	10 kWth	coke, coal	2010	34
Bidwe et al.	Stuttgart	10 kWth	syngas	2011	35
Thon et al.	Hamburg	25 kWth	coal	2012	36
Pilot Dual Fluidized Beds Plant					
Markström et al.	Chalmers	100 kWth	coal	2012	37
Kolbitsch et al.	Vienna	120 kWth	H_2, CO, CH_4	2010	7
Galloy et al.	Darmstadt	1 MWth	coal	2011	8

[a]Year when the work was published. [b]Instituto de Carboquímica (CSIC).

It can be clearly seen from Table 1 that most experiments were conducted using ilmenite as the oxygen carrier in different reactors, from lab-scale test facilities, such as TGA, fixed bed, and batch fluidized bed, to 10 kWth interconnected fluidized bed reactor, and finally to 100 kWth to 1 MWth scale pilot units. The reported positive results on almost all the facilities indicate that ilmenite is a potential and promising material for CLC. The main issue with ilmenite is its low reactivity. The reduction rate of ilmenite with CO was about 1.6%/min.[25] Even though ilmenite can increase its reactivity with the cycles, the reduction rate of activated ilmenite with CO was only 2.5%/min.[38] Compared to the reactivity of the synthetic carriers, 6.6 and 18.2%/min for Fe- and Ni-synthetic carriers with CO, respectively,[38] ilmenite shows a much lower reactivity. This low reactivity results in a large bed inventory and a high pressure drop in the fuel reactor. According to the comparison among different low-cost Fe-based oxygen carriers done by Abad et al,[39] the required bed inventory for ilmenite in the fuel reactor is about 8−10 times that required for the synthetic Fe-based oxygen carrier. In addition, the low reactivity causes the incomplete gas conversion and reduces the conversion ratio of carbon. For example, the test of ilmenite with coal in the 10 kWth chemical-looping combustor in Chalmers[33] and the 500 Wth unit in CSIC[32] demonstrated that there was 20% unconverted gas (CO, H_2, and CH_4) leaving the fuel reactor. Therefore, increasing the reactivity of ilmenite is necessary and important for the development of CLC technology; this concept motivates the present paper.

The activation process for ilmenite has already been found during consecutive redox cycles.[25,26,30] The principle of faster reactivity after activation is based on the porosity increase of the ilmenite particle. Although the activation process can increase the reactivity, the activation is slow if the reduction conversion is low. For example, it takes as long as 30 cycles for 1 min reduction with CH_4.[25] Moreover, the reactivity rise after activation is still limited, compared to the synthetic oxygen carriers, as mentioned previously. Considering that the reactivity gained from activation is because of pore formation, one possible method to improve the reactivity is to further develop the pore structures. The formation of pores during activation comes from the diffusion of the iron and oxygen ions.[40] Therefore, when considering the promotion of pore formation, increasing the diffusion rate of ions can be a solution. Alkali- and alkaline earth metals, such as potassium (K), sodium (Na), and calcium (Ca), are already well-known for their self-diffusion properties.[41,42] The improvement of natural ilmenite reactivity by introducing foreign alkali- and alkaline metal ions, such as K^+, Na^+, and Ca^{2+}, has not been reported yet.

Accordingly, the present research was aimed at promoting the reactivity of ilmenite by introducing foreign ions. The effects of different foreign ions (K^+, Na^+, and Ca^{2+}) and different loading amounts of foreign ions on the reduction reactivity of ilmenite were investigated. The probable mechanism of the effect of foreign ions on ilmenite's reactivity has been proposed as well.

2. EXPERIMENTAL SECTION

2.1. Preparation and Characterization of the Ilmenite.

The ilmenite used in this work was supplied by Wogen Plc, Guangzhou Branch. The received ilmenite particles were first heat treated in air for 24 h at 950 °C to obtain ilmenite in its most oxidized state.[28] The calcinated particles were then sieved to 125−200 μm. The Brunauer−Emmett−Teller (BET) area of the calcinated ilmenite particles is 0.64 m^2/g. The calcined ilmenite particles are defined as the raw ilmenite in this study. X-ray fluorescence (XRF) analysis reveals that the raw ilmenite contains 50.54% TiO_2, 42.32% Fe_2O_3, 2.32% SiO_2, 1.98% MnO, 1.45% Al_2O_3, and some other minor phases. X-ray diffraction (XRD) shows that Fe_2TiO_5 and TiO_2 are the major components, with a minor amount of Fe_2O_3.

The foreign ions were added to the raw ilmenite based on the wet impregnation method employed by Yang et al.[43] K_2CO_3, Na_2CO_3, and $Ca(NO_3)_2{\cdot}4H_2O$ (purity > 99.9 wt %; size < 5 μm) were employed as the precursors. The precursor was dissolved in 100 mL deionized water, to give an approximately 4 M solution. The raw ilmenite, prepared as described above, was soaked in the solution. The mixture of the

dx.doi.org/10.1021/ie400237p | Ind. Eng. Chem. Res. 2013, 52, 6119−6128

precursor and ilmenite was stirred for 24 h at ambient temperature and dried in air at 393 K. The dried product of K_2CO_3 or Na_2CO_3 impregnated ilmenite was cooled in air and then resieved to 125−200 μm directly. The dried Ca-$(NO_3)_2{\cdot}4H_2O$ impregnated ilmenite was first heated at 900 °C for 1 h to release NO_x, then cooled down to room temperature in air, and finally resieved to 125−200 μm. The mass ratio of the foreign metal ion to ilmenite (metal/ilmenite) was controlled during preparation. Three mass ratios of K/ilmenite, 5 wt %, 10 wt %, and 15 wt %, were chosen, while only one mass ratio of Na and Ca/ilmenite 10 wt % was specified. For simplicity, the final products were designated as K5-ilmenite, K10-ilmenite, K15-ilmenite, Na10-ilmenite, and Ca10-ilmenite.

2.2. Apparatus. Experiments were conducted in a laboratory-scale fluidized bed reactor of quartz with I.D. 30 mm, heated by an external furnace, with the temperature monitored by a K-type thermocouple. For all the experiments except when the bed inventory was a variable parameter, a sample of ∼50 g of ilmenite particles of size 125−200 μm was placed on the porous plate. The bed height was about 27 mm when the bed was not fluidized. The flow rate of the fluidizing gas was 2 L/min (STP), which gave U/U_{mf} = 3.07 at 900 °C, where the minimum fluidizing velocity U_{mf} was calculated.[44] All the product gas went into a gas analyzer after passing through a filter that recovered the solids elutriated from the fluidized bed. The bed material was first heated under air atmosphere to the reaction temperature 900 °C, in order to thermally decompose the metal carbonate K_2CO_3 or Na_2CO_3 completely, and make certain that the ilmenite was in its most oxidized state. In each cycle, ∼11 vol % CO was used to reduce the bed material at 900 °C for 5 min, and 5.5 vol % O_2 (air diluted by nitrogen) was introduced for a full oxidation at 840 °C. Between these two periods, nitrogen was fed into the bed for 3 min to purge. Each sample underwent 40 continuous redox cycles. The use of lower temperature (840 °C) and diluted air (5.5 vol % O_2) during oxidation was to avoid the temperature rise due to the exothermal oxidation reaction. Thermodynamically, further reducing Fe_2TiO_5 and Fe_2O_3 in ilmenite past $FeTiO_3$ and Fe_3O_4 will cause the incomplete conversion of the reducing gases such as CO and H_2, which is not suitable for CLC. In this study, Fe_2TiO_5 and Fe_2O_3 are only reduced to $FeTiO_3$ and Fe_3O_4 by mass balance verification.

The initial oxygen carrier particle and the one after 40 cycles were characterized by several techniques. The BET surface area and pore volume of the particles were measured with a Micromeritics micropore analyzer (Autosorb-iQ2-MP, NOVA4000). The particles were fixed by resin and then ground with the abrasive paper (Grit No. CW 2000) to obtain the cross section. The cross section morphology of the ground particles was observed under a scanning electron microscope (SEM, JSM-7001F). SEM-energy dispersive spectrometer (EDS) was performed to analyze the element distribution. The crystalline chemical species was probed by a powder X-ray diffraction (XRD, D/maxIIIB).

2.3. Data Evaluation. The rate of oxygen transferred $r_o(t)$ (mol/s) can be obtained from the gas product distribution. Equations 1 and 2 give the rate of oxygen transferred from ilmenite to the fuel during reduction and that from oxygen in the air to ilmenite during oxidation, respectively.

For reduction:

$$r_o(t) = (x_{CO_2})_{out}F_{out} - (x_{CO_2})_{in}F_{in} \quad (1)$$

For oxidation:

$$r_o(t) = 2(x_{O_2})_{in}F_{in} - 2(x_{O_2})_{out}F_{out} \quad (2)$$

where F_{in} and F_{out} (mol/s) are the molar flow rates of the inlet and outlet gas streams, and x_i is the molar fraction of the gas species i.

The oxygen yield γ_o is defined as the oxygen gained for the fuel from ilmenite divided by the oxygen needed for complete oxidation of the fuel, as given by eq 3. γ_o denotes the instant extent the fuel has been oxidized by the oxygen carrier during reduction.

$$\gamma_o(t) = \frac{r_o(t)}{(x_{CO})_{in}F_{in}} \quad (3)$$

The mass based conversion of ilmenite ω, indicating the real oxygen transferred, can be calculated from eq 4 and eq 5.

For reduction:

$$\omega(t) = 1 - \frac{M_O}{m_{ox}}\int_{t_0}^{t} r_o(t)\,dt \quad (4)$$

For oxidation:

$$\omega(t) = \omega_{f,red} + \frac{M_O}{m_{ox}}\int_{t_0}^{t} r_o(t)\,dt \quad (5)$$

where M_O (kg/mol) is the molar mass of oxygen. m_{ox} (kg) is the mass of ilmenite in the most oxidized form. t_0 (s) is the reaction onset time. $\omega_{f,red}$ is the final conversion of ilmenite in the previous reduction.

3. RESULTS AND DISCUSSION

3.1. Reactivity of the Raw Ilmenite. The behavior of the raw ilmenite during continuous 40 redox cycles was investigated in the fluidized bed reactor. As an example, Figure 2a shows the off-gas distribution for the first cycle. CO_2 is formed immediately after introducing the reducing gas; however, conversion of the reducing gas is not complete. The unconverted CO is up to 8 vol % for the first cycle. Figure 2b represents the outlet CO and CO_2 concentrations during reduction for the successive 40 cycles. It can be seen that the product CO_2 concentration increases gradually with each cycle, while the unconverted CO decreases correspondingly. The comparison of the product gas distribution and the oxygen yield among different cycles (cycles 1, 5, 10, 20, 30, and 40) can be found in Figure 3. Figure 3 clearly shows the gradual decrease of the CO concentration and the increase of the CO_2 concentration with the number of cycles during the 40 cycles. The reason for this is that ilmenite experiences the activation process that increases its reactivity, resulting in more CO being converted into CO_2. For cycle 40, the CO_2 concentration reaches the maximum 5.44 vol % with the minimum unconverted CO 5.56 vol %. The reactivity enhancement results in a deeper reduction extent under the same experimental condition, corresponding to a reduced conversion ω of ilmenite, as shown in Figure 3d. The reduced conversion of ilmenite results in a longer time for oxidization due to the increase of ω for oxidation (see in Figure 3c). Moreover, the oxygen yield increased with the gain in reactivity over the cycles (see Figure 3d).

dx.doi.org/10.1021/ie400237p | Ind. Eng. Chem. Res. 2013, 52, 6119−6128

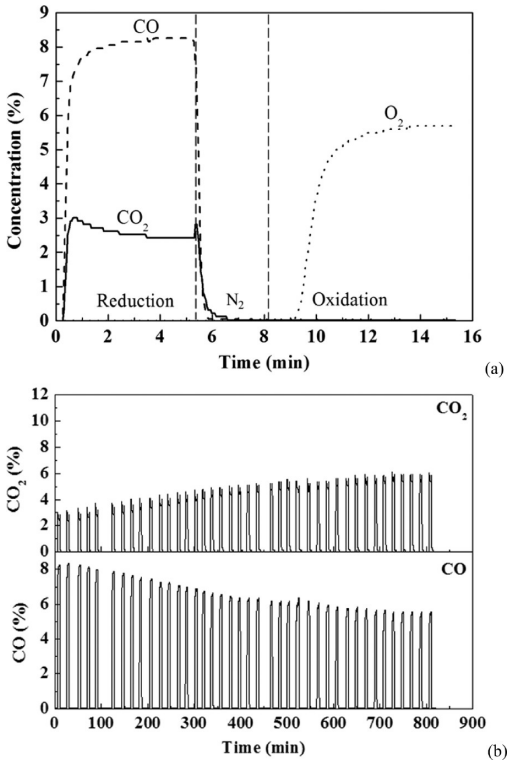

Figure 2. The CO_2, CO, and O_2 concentrations in the off-gas for (a) the 1st cycle; (b) the successive 40 redox cycles with ~50 g raw ilmenite as the bed material. The O_2 concentration during oxidation was not shown in panel b.

3.2. Effect of Foreign Ion Type on the Reduction of Ilmenite. After the reactivity study of the raw ilmenite, ilmenite impregnated with 10 wt % K, 10 wt % Na, and 10 wt % Ca, namely K10-ilmenite, Na10-ilmenite, and Ca10-ilmenite, was investigated in order to understand the effect of different foreign ions on the reduction reactivity of ilmenite. Figure 4 shows the outlet CO and CO_2 concentrations over 40 cycles for the reduction of K10-ilmenite, Na10-ilmenite, and Ca10-ilmenite. The addition of all the three foreign ions leads to less remaining CO and more CO_2 generated, comparing to the raw ilmenite case in Figure 2b. For example, in the 20th cycle, the unconverted CO fraction is 1.22 vol % for K10-ilmenite, 2.31 vol % for Na10-ilmenite, 4.51 vol % for Ca10-ilmenite, but up to 6.36 vol % for the raw ilmenite. The reactivity enhancement during the ilmenite reduction in the presence of foreign ions is quite significant. Meanwhile, the effect of foreign ions on enhancing the reduction reactivity of ilmenite is in the sequence of $K^+ > Na^+ > Ca^{2+}$. The reactivity of ilmenite impregnated with foreign ions also changes over the cycles. On the beginning of several cycles, there is a small increase for the unconverted CO concentration with each cycle, except during the first cycle of Na10-ilmenite. After the first 3 cycles for K10-ilmenite, 4 cycles for Na10-ilmenite, and 13 cycles for Ca10-ilmenite, the unconverted CO concentration starts to decrease gradually, and then remains stabilized from cycle 12 for K10-ilmenite, cycle 16 for Na10-ilmenite, and cycle 28 for Ca10-ilmenite. Accordingly, as the redox cycle continues, the reactivity of the modified ilmenite experiences a small decrease at first, then increases gradually, and finally becomes stabilized.

Figure 5 represents the comparison of product gas distribution with time and the oxygen yield with the mass based conversion between the first cycle and the 40th cycle for K10-ilmenite, Na10-ilmenite, and Ca10-ilmenite. Note here that the result of cycle 40 is representative of the cycles when the reactivity becomes stabilized. To be specific, cycle 40 represents cycles 12−40 for K10-ilmenite, cycles 16−40 for Na10-ilmenite, and cycles 28−40 for Ca10-ilmenite. Reduction

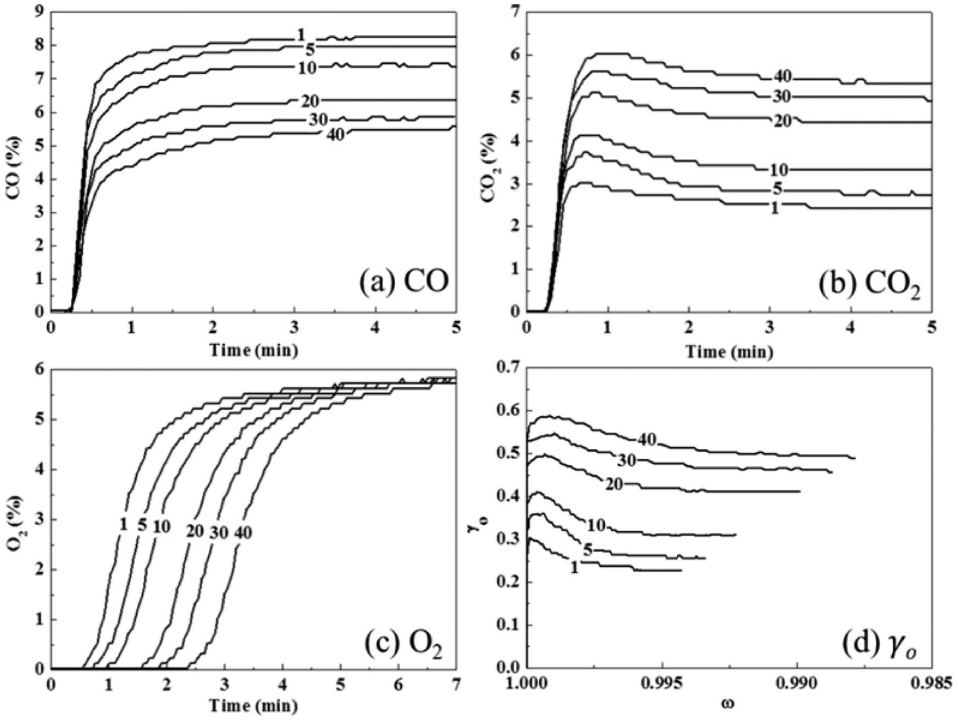

Figure 3. The CO, CO_2, O_2 concentrations with time and the oxygen yield γ_o with mass based conversion of ilmenite ω for cycle 1, 5, 10, 20, 30, 40 with ~50 g raw ilmenite as the bed material.

dx.doi.org/10.1021/ie400237p | Ind. Eng. Chem. Res. 2013, 52, 6119−6128

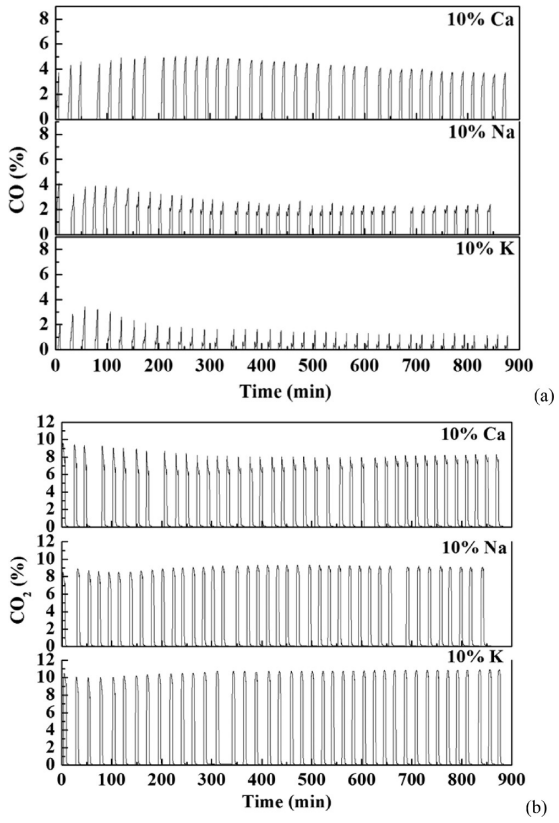

Figure 4. The (a) CO and (b) CO_2 concentrations in the off-gas during reducing the ilmenite impregnated with 10% K, 10% Na, and 10% Ca over 40 redox cycles. Bed inventory: ~50 g.

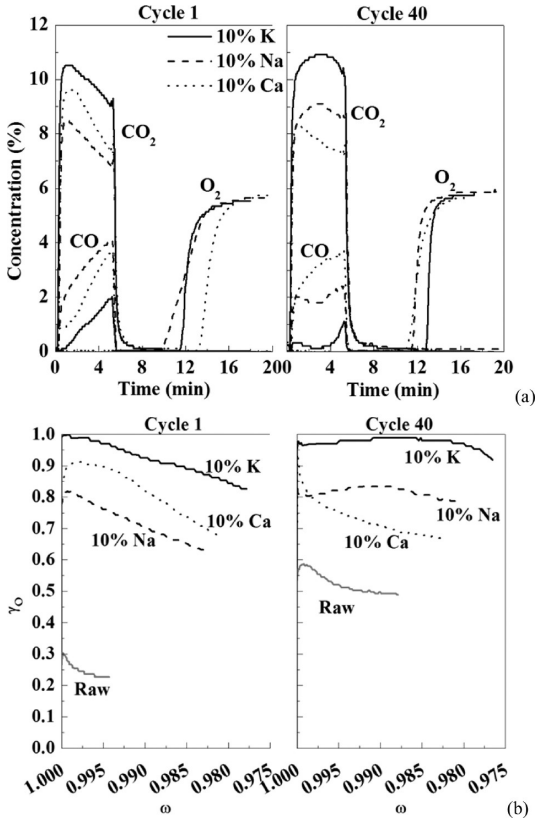

Figure 5. Comparison of (a) the product gas distribution with time and (b) oxygen yield γ_o with mass based conversion ω between the 1st cycle and the 40th cycle for reducing the ilmenite impregnated with 10% K, 10% Na, and 10% Ca. Bed inventory: ~50 g.

reactivity increases after 11 cycles for K10-ilmenite and after 15 cycles for Na10-ilmenite, which results in a lower CO concentration, a higher CO_2 concentration, a longer time needed for oxidation (Figure 5a), and a higher oxygen yield (Figure 5b). Meanwhile, the reactivity of the K10-ilmenite after 11 cycles or Na10-ilmenite after 15 cycles becomes more stable within the 5 min reduction period, in comparison to the continuous decrease in cycle 1. However, this is a different case for Ca10-ilmenite. The reactivity of Ca10-ilmenite at cycle 40 decreases at the start of the reduction, but remains nearly the same value as in cycle 1 when reduction ends. Hence, the change of Ca10-ilmenite's reactivity over 40 cycles could be neglected. In Figure 5b, the ilmenite impregnated with K^+, Na^+, or Ca^{2+} shows a higher oxygen yield with a reduced conversion than the raw ilmenite in cycle 1 and the stabilized cycles. This further confirms the reactivity enhancement effect by the addition of foreign ions as discussed previously. The effect of foreign ions on improving the reactivity is in the sequence of $K^+ > Ca^{2+} > Na^+$ for the first cycle and $K^+ > Na^+ > Ca^{2+}$ for the stabilized cycles. For K10-ilmenite, the oxygen yield reaches nearly 1.0 and less than 0.92 vol % CO is detected at the outlet. It can be seen that, among the three types of ilmenite impregnated with K^+, Na^+, and Ca^{2+}, K10-ilmenite shows the best performance during the 40 cycles. In other words, compared with Na^+ and Ca^{2+}, K^+ is the best foreign ion for enhancing the reduction reactivity of ilmenite.

3.3. Effect of K^+ Loading Amount on the Reduction of Ilmenite. After the best foreign ion K^+ has been found, the effect of the K^+ loading amount (i.e., the mass ratio of K^+) on the reduction behavior of ilmenite becomes an interesting issue. It is meaningful to find the influence of K^+ loading amount on the reactivity of ilmenite. Figure 6 shows the outlet CO and CO_2 concentration over 40 redox cycles for the ilmenite impregnated with 5 wt % K, 10 wt % K, and 15 wt % K, that is, K5-ilmenite, K10-ilmenite, K15-ilmenite. In comparison to the off-gas distribution of the raw ilmenite in Figure 2b, the off-gas, for the three ilmenite with different amounts of K^+, is composed of less unconverted CO and more CO_2 over 40 cycles, indicating a reactivity rise by the addition of K^+. The effect of different amounts of K^+ on increasing the reactivity of ilmenite is in the sequence of 15 wt % K^+ > 10 wt % K^+ > 5 wt % K^+. It takes 11 cycles for these three K^+-impregnated ilmenite samples to stabilize. After 11 cycles, both K15-ilmenite and K10-ilmenite show a high CO conversion, with the remaining CO at the outlet being as little as 0.42 vol % for K15-ilmenite and 0.92 vol % for K10-ilmenite at the 40th cycle. However, the reactivity of K5-ilmenite is proven to be much slower than K10-ilmenite and K15-ilmenite. The unconverted CO in the last cycle for K5-ilmenite is up to 5.10 vol %, which is near the amount 5.56 vol % for the raw ilmenite.

Figure 7 compares the off-gas distribution and the oxygen yield in the 40th cycle with that in the first cycle for K5-ilmenite, K10-ilmenite, and K15-ilmenite. Here, cycle 40 represents all the stabilized cycles, that is, cycle 12−40. It can be found that there is an increase of CO_2 concentration and oxygen yield with a decrease of CO concentration after 11 cycles for both K10-ilmenite and K15-ilmenite, corresponding to a faster reactivity. The reactivity of K15-ilmenite is a little slower than K10-ilmenite at the initial first cycle. However, after 11 cycles, K15-ilmenite and K10-ilmenite tend to obtain a similar reactivity, with K15-ilmenite being a little faster than

dx.doi.org/10.1021/ie400237p | Ind. Eng. Chem. Res. 2013, 52, 6119−6128

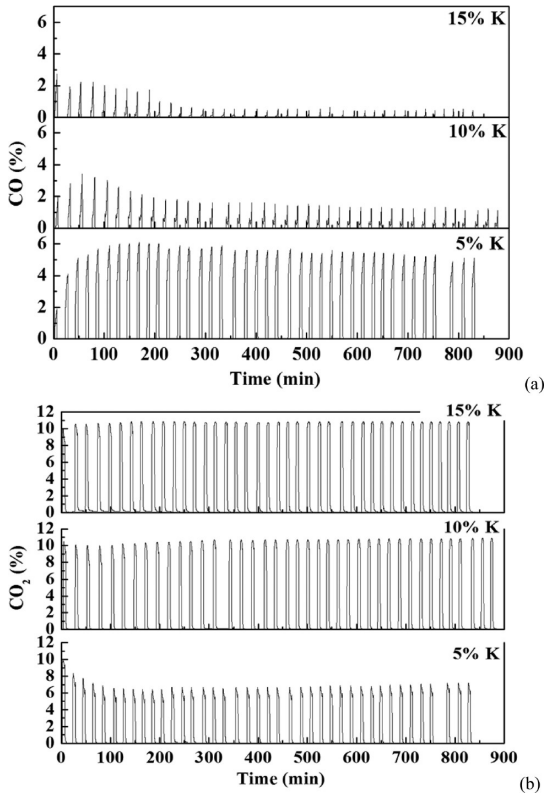

Figure 6. The (a) CO and (b) CO_2 concentrations in the off-gas during reducing the ilmenite impregnated with 5% K, 10% K, and 15% K over 40 redox cycles. Bed inventory: ~50 g.

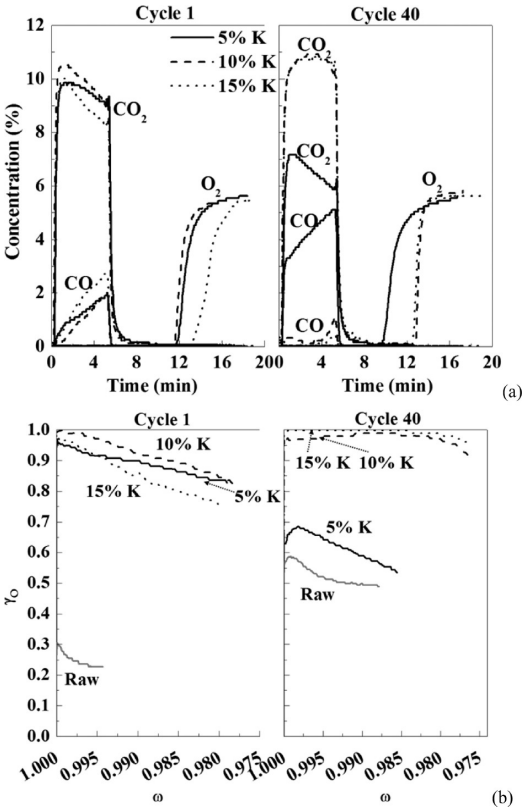

Figure 7. Comparison of (a) the product gas distribution with time and (b) oxygen yield γ_o with mass based conversion ω between the 1st cycle and the 40th cycle for reducing the ilmenite impregnated with 5% K, 10% K, and 15% K. Bed inventory: ~50 g.

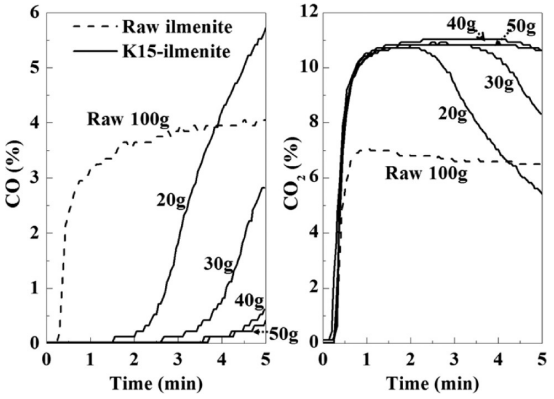

Figure 8. The CO and CO_2 concentrations in the off-gas during the reduction of the raw ilmenite (100 g) and K15-ilmenite with different bed inventories (20, 30, 40, and 50 g). Both the raw ilmenite and K15-ilmenite have already experienced 40 cycles and have a stable reactivity.

K10-ilmenite. The reactivity of K15-ilmenite or K10-ilmenite continues to decrease at the first cycle, and then after 11 redox cycles a much more stable reactivity is gained. Also a nearly complete CO conversion and a high oxygen yield (0.92−1) can be achieved for both K10-ilmenite and K15-ilmenite after 11 cycles. Nevertheless, K5-ilmenite, a less loading amount of K^+, shows a decrease in reactivity after 11 cycles, with more CO and less CO_2 appearing at the outlet and a lower oxygen yield. In a word, the best loading ratio of K^+ to ilmenite is 15 wt % from the experiments. Regardless of the difference between these three kinds of ilmenite impregnated with different ratios of K^+, the foreign ion K^+ addition does significantly increase the reactivity of the raw ilmenite (see Figure 7b).

3.4. Effect of the Bed Inventory. From the above discussion, K15-ilmenite has been proven to have the most enhanced reduction reactivity. It should be noted that ~50 g of oxygen carrier was used in the above experiments. Figure 7 denotes that 50 g of K15-ilmenite is excess for a kinetic behavior study, because the outlet CO fraction is very low. To effectively study the reactivity of K15-ilmenite, its bed inventory was reduced while other conditions remained unchanged. At the same time, for comparison, the bed inventory of the raw ilmenite was increased to 100 g. Figure 8 illustrates the off-gas composition during the reduction of the raw ilmenite (100 g) and K15-ilmenite with different bed inventories (20 g, 30 g, 40 g, and 50 g). Here, the raw ilmenite or K15-ilmenite has experienced 40 cycles and a stable reactivity has been obtained. In the case of K15-ilmenite, a complete conversion of CO can be achieved even with 20 g of bed inventory. The subsequent rise of the CO concentration was a result of the deep reduction past $FeTiO_3$ and Fe_3O_4. Here, we only focus on the reactivity in the beginning period when CO was fully oxidized into CO_2. The duration for a complete CO conversion became shorter as the K15-ilmenite bed inventory decreased. Even so, a full conversion of CO can be maintained for as long as ~2 min with only 20 g of K15-ilmenite. However, even when the bed mass for the raw ilmenite was increased to 100 g, there was still 4.05 vol % CO in the off-gas. The required bed inventory for a complete CO conversion is 14.39 g/vol % CO for the raw ilmenie and only 1.82 g/vol % CO for K15-ilmenite, which is approximately 8 times less. Theoretically, the required bed

dx.doi.org/10.1021/ie400237p | Ind. Eng. Chem. Res. 2013, 52, 6119−6128

inventory is inversely proportional to the conversion rate of the oxygen carrier.[4] Accordingly, the reactivity of K15-ilmenite is ~8 times faster than the raw ilmenite. The study by Mendiara et al.[38] states the reaction rate of the activated ilmenite as 2.5%/min. Hence, the reaction rate of K15-ilmenite is 20%/min, which is approximately equivalent to the rate of the synthetic Ni-based carrier (18.2%/min[38]). Correspondingly, the required bed inventory for K15-ilmenite will be in the identical range as for the synthetic Ni-based carrier. The performance of the natural ilmenite has been successfully improved to the level of the synthetic carrier. This is a significant progress for the ilmenite.

3.5. Sintering and Agglomeration. Particle sintering and agglomeration must be avoided because this can lead to defluidization that causes solid circulation disturbances and influences the gas−solid contact. For all the experiments in this work, sintering of the particles or agglomeration of the fluidized bed was never observed. Particles extracted from the fluidized bed at the end of each experiment did not show evidence of agglomeration. In fact, porous structures were formed after 40 cycles. The structure transition will be discussed in section 3.6. The maximum extent of reduction for all the tests corresponds to the mass based conversion ω = 0.977 (50 g of bed inventory), and ω = 0.951 (20 g of bed inventory). At this conversion range, theoretically, only 0.18−0.96 wt % free Fe_2O_3 could be reduced to FeO, with most Fe_2O_3 being reduced to Fe_3O_4. FeO formation should be avoided in CLC because of both thermodynamic limitations and agglomeration induction.[45] Therefore, in the conversion range suitable for the CLC system, the ilmenite impregnated with foreign ions has no problem of sintering or agglomeration.

3.6. Characterization of the Oxygen Carriers. To explain the effect of foreign ions on increasing the reactivity of ilmenite, morphological characterizations of the initial oxygen carrier particle and the one after 40 redox cycles in the fluidized bed were performed by SEM. Since ilmenite is a natural ore, it has a heterogeneous structure. Hence, during the SEM test, all the cross-cut particles of each batch were observed. All the particles show a similar morphological character. Figure 9, as a representative, shows the cross section morphology of different ilmenite particles tested in this work. The initial raw ilmenite presents a solid structure (Figure 9a-i). After 40 cycles, the raw ilmenite shows a slight gain in porosity at the outer edge, whereas the inner solid texture remains consistent (Figure 9a-ii). This occurrence is the reason for the reactivity increase after the activation period.

The ilmenite impregnated with different types of foreign ions at different ratios maintained the same solid structure as initial raw ilmenite in Figure 9a-i. There are structural changes after continuous 40 cycles for these modified ilmenites. Figure 9 panels b−d display the cross sectional morphologies of the cycled ilmenite with different types of foreign ions, i.e., K10-ilmenite, Na10-ilmenite, and Ca10-ilmenite. It is clear that different pore structures are formed after 40 cycles. A uniform porous appearance throughout the whole cross section of K10-ilmenite can be found in Figure 9b. Similarly, there is also a porous structure formed for Na10-ilmenite; however, the porous structure for the cycled Na10-ilmenite is less uniform, with solid parts being scattered among the pore spaces (Figure 9c). The porosity of the Ca10-ilmenite after 40 cycles is even less ideal; the porous structure is only found around the outer edge while the inner core remains solid with only several cracks (Figure 9d). Figure 9 panels e and f show the cross sectional

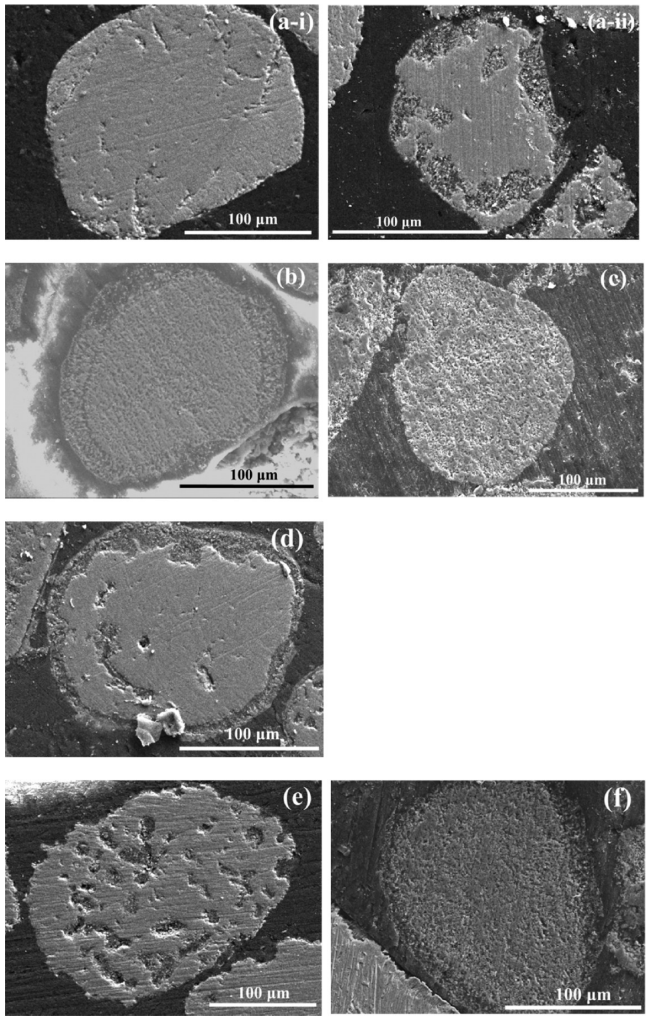

Figure 9. Cross sectional SEM images of ilmenite particles. (a-i) initial raw ilmenite; (a-ii) raw ilmenite, (b) K10-ilmenite, (c) Na10-ilmenite, (d) Ca10-ilmenite, (e) K5-ilmenite, (f) K15-ilmenite after 40 cycles.

morphologies of K5-ilmenite and K15-ilmenite. K5-ilmenite, a small loading amount of K^+, has some macropores or cracks formed in the cross section after 40 cycles, with most parts remaining solid (Figure 9e). However, ilmenite with a larger loading amount of K^+, such as K10-ilmenite or K15-ilmenite, obtains a uniform, porous structure after 40 cycles (Figure 9b,f). The surface area and pore volume of the modified ilmenite tend to increase as the K^+ loading amount increases, as given in Figure 10. After 40 cycles, K10-ilmenite and K15-ilmenite obtain a larger surface area and pore volume than K5-ilmenite and the raw ilmenite. The cycled K15-ilmenite forms the best structure; its BET surface (1.27 m^2/g) and pore volume (4.63×10^{-6} m^3/kg) are approximately 4 times that of the activated raw ilmenite.

The different pore structures correspond with the reactivity differences. The modified ilmenite represents more pores or cracks than the activated raw ilmenite. This clearly shows that the addition of foreign ions can indeed assist in developing the pore structures of the ilmenite particle. Because of this, the modified ilmenite obtains a faster reactivity than the raw ilmenite. Among the ilmenite impregnated with different types of foreign ions, the porosity is in the sequence of K10-ilmenite > Na10-ilmenite > Ca10-ilmenite, which agrees with the reactivity sequence, as discussed in 3.2. Likewise, as to the

dx.doi.org/10.1021/ie400237p | Ind. Eng. Chem. Res. 2013, 52, 6119−6128

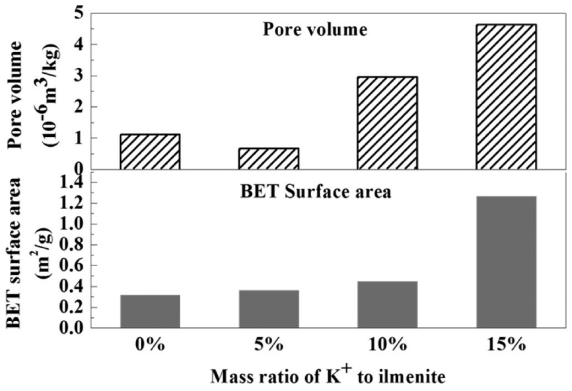

Figure 10. BET surface area and pore volume as a function of the mass ratio of K^+ to ilmenite for the raw ilmenite, K5-ilmenite, K10-ilmenite, and K15-ilmenite. All the particles experienced 40 cycles.

ilmenites with different loading amounts of K^+, both K10-ilmenite and K15-ilmenite form a more uniform, porous structure than K5-ilmenite does. This is the reason for a faster reactivity of K10-ilmenite or K15-ilmenite, as represented in 3.3.

The foreign ion distribution throughout the cross-cut ilmenite particles was detected by EDS. In each batch for the EDS test, several particles and different locations of each particle were analyzed. The data is in the same range and also exhibits the same trend. Table 2 lists the mole fractions of foreign ions at different locations of the cross-cut particle. Higher percentages of foreign ions are assembled at the surface of the particle initially. At the end of 40 cycles, the distribution of foreign ions for ilmenite added with K^+ or Na^+ is changed: a larger proportion of K or Na appears at the internal edge and center; a relatively smaller percentage remains at the outside surface. This redistribution suggests that there is diffusion of K^+ or Na^+ from the external, highly loaded region to the internal part with the redox cycles. To keep the particle electrically neutral, during the diffusion of K^+ or Na^+, there must be a vacancy carrying the same amount of electric charge diffusing in the opposite direction. This process is classical Krikendall effect in metallurgy.[46] Condensation of excess vacancies results in the void or pore formation near the original interface and within the fast-diffusion side.[47] The high-frequency diffusion of K^+ or Na^+ aids the development of the pore structure inside the particle. From this point, K^+ or Na^+ acts as a "pore promoter". The pore formation reduces the internal gas diffusion resistance and increases the gas–solid contact area, thus increasing the ilmenite reactivity. Once the uniform porous structure of ilmenite is formed, a fast reactivity is obtained and will be maintained. Different from K^+ or Na^+, Ca^{2+} exists only on the external surface of Ca10-ilmenite either before cycling or after 40 cycles, which shows no redistribution. This indicates that it is difficult for Ca^{2+} to diffuse inside ilmenite lattice. This situation is why Ca10-ilmenite has a slower reactivity than K10-ilmenite or Na10-ilmenite.

Figure 11 shows the XRD profiles of the raw ilmenite, K10-ilmenite, Na10-ilmenite, and Ca10-ilmenite before the experiments and after 40 redox cycles. There is existence of hematite Fe_2O_3 and titanium dioxide TiO_2 in all the tested particles. Fe_2TiO_5 only exists in the unreacted particles and the cycled raw ilmenite, but not in the cycled, impregnated ilmenite particles. In the initial impregnated ilmenite, the foreign ions, that is, K^+, Na^+, and Ca^{2+}, are physically adsorbed in the forms of K_2CO_3, Na_2CO_3, and CaO respectively. K_2CO_3 and Na_2CO_3 undergo thermal decomposition and generate K_2O and Na_2O before starting the first cycle. After 40 cycles, however, alkali-rich phases formed between foreign ions and titanium or iron oxides, $K_{1.46}Ti_{7.2}Fe_{0.8}O_{16}$, $Na_2Fe_2Ti_6O_{16}$, and $CaTiO_3$, are detected. This indicates that a fraction of the physical adsorbed foreign ions reacts with the components of the ilmenite. The alkali-rich phases are generated through chemical reactions. The EDS analysis for the K15-ilmenite particles after 70 and 100 cycles (not given in Table 2) shows that the mole fraction of K^+ or Na^+ does not vary much after 40 cycles (see Table 2). This means that the alkali-rich phases formed are quite stable. The chemical combination of the alkali-rich phases together with the segregation of Fe_2O_3 from the titanium-rich phase, as reported in the literature,[25,48] results in the loss of Fe_2TiO_5 in the cycled, impregnated ilmenite. Muhler et al[49]. reported that the potassium iron oxide $KFeO_2$ was a catalytically active phase, which could lower the activation barrier. Therefore, the alkali-rich phase could also behave as an active phase that can further promote pore development and increase reactivity. However, more research is needed to demonstrate the activity of the

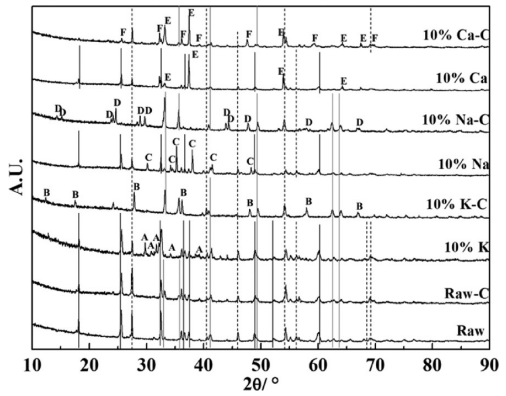

Figure 11. XRD patterns for the raw ilmenite (raw), K10-ilmenite (10% K), Na10-ilmenite (10% Na), and Ca10-ilmenite (10% Ca). "–C" denotes the material after 40 cycles in the fluidized bed: (dark solid line) Fe_2TiO_5; (light solid line) Fe_2O_3; (dashed line) TiO_2. (A) K_2CO_3; (B) $K_{1.46}Ti_{7.2}Fe_{0.8}O_{16}$; (C) Na_2CO_3; (D) $Na_2Fe_2Ti_6O_{16}$; (E) CaO; (F) $CaTiO_3$.

Table 2. The Foreign Ion Distribution for the Cross-Cut Ilmenite Particles Analyzed by EDS. Mole Fractions of Foreign Ions at Different Locations of the Initial Particle and the Particle at the End of 40 Cycles Are Listed

	K10-ilmenite		Na10-ilmenite		Ca10-ilmenite		K5-ilmenite		K15-ilmenite	
mole fractions (%)	initial	end	initial	end	initial	end	initial	end	initial	end
surface	8.46	0.26	2.13	1.69	1.4	0.52		0.42		1.34
edge	0.89	2.11	0	2.62	0	0		1.41		4.27
center	0.66	2.03	0	3.21	0	0		0.57		3.46

dx.doi.org/10.1021/ie400237p | Ind. Eng. Chem. Res. 2013, 52, 6119–6128

alkali-rich phase in the future. Moreover, Table 2 shows that the foreign ion concentration on the surface is relatively low at the end of 40 cycles. A fractional loss of the foreign ions during the transition from the initial alkali carbonates to the alkali-rich phases is due to the volatility of the alkali metals under the reaction condition. The released alkali metals will be carried downstream by the gas phase and cause problems, for example, deposition and corrosion. To avoid these downstream problems, additives, such as kaolin,[50] SiO_2, MgO, and Al_2O_3,[51] can be used to capture the released alkali metals. However, the volatilization of the alkali metals mostly occurs during the transition from K_2CO_3 or Na_2CO_3 to the alkali-rich phase. The formation of the stable alkali-rich phase can inhibit volatilization. With regard to this aspect, the impregnated ilmenite can complete the alkali metal volatilization process in a separate laboratory scale fluidized bed reactor before participating in the real reaction.

4. CONCLUSIONS

In this work, the reduction reactivity of the natural ilmenite oxygen carrier was promoted successfully by the introduction of foreign ions. The modified ilmenite was prepared by impregnating K_2CO_3, Na_2CO_3, or $Ca(NO_3)_2$ into the raw ilmenite particle. The reduction reactivity and cyclic stability of the modified ilmenite were studied in a fluidized bed reactor. The following conclusions can be drawn.

(1) The reduction reactivity of ilmenite can be enhanced by introducing three different types of foreign ions − K^+, Na^+, Ca^{2+}. The efficacy of increasing the reactivity is in the sequence of $K^+ > Na^+ > Ca^{2+}$.

(2) The effect of K^+ loading amount on improving the reactivity has the sequence of 15 wt % K^+ > 10 wt % K^+> 5 wt % K^+. Ilmenite added with 10 wt % or 15 wt % K^+ shows a much faster reactivity than that with only 5 wt % K^+. The optimum loading ratio of K^+ to ilmenite is 15 wt % from this study.

(3) The 15 wt % K^+ modified ilmenite's surface area and pore volume increases by ∼4 times, and its reactivity increases ∼8 times over the activate raw ilmenite. This reactivity is in the same level as the synthetic Ni-based carrier. The required bed inventory in the fuel reactor will thus be reduced to the amount used with the synthetic Ni-based carrier.

(4) The migration or diffusion of K^+ and Na^+ helps promote the pore structure and thus increases the surface area and the pore volume. The detected alkali-rich phase, i.e., $K_{1.46}Ti_{7.2}Fe_{0.8}O_{16}$ or $Na_2Fe_2Ti_6O_{16}$, is most likely an active phase for pore development. The pore promoting effect and the formation of the active alkali-rich phase are possible mechanisms for the reactivity enhancement effect of foreign ions on ilmenite. Ca^{2+} has a weak effect on enhancing the reactivity because of its slow diffusion rate.

AUTHOR INFORMATION

Corresponding Author

*Tel.: 86-10-62781741. Fax: 86-10-62770209. E-mail: lizs@mail.tsinghua.edu.cn.

Notes

The authors declare no competing financial interest.

ACKNOWLEDGMENTS

This work was supported by National Natural Science Foundation of China (51061130535), the National Key Basic Research and Development Program (2011CB707301), Tsinghua University Initiative Scientific Research Program, and Program for New Century Excellent Talents in University (NCET-12-0304).

NOMENCLATURE

F_{in} = molar flow rate of the inlet gas stream (mol/s)
F_{out} = molar flow rate of the outlet gas stream (mol/s)
M_O = molar mass of oxygen (kg/mol)
m_{ox} = mass of the oxygen carrier in its most oxidized form (kg)
$r_o(t)$ = rate of oxygen transferred (mol/s)
t_0 = reaction onset time (s)
U = superficial fluidizing gas velocity (m/s)
U_{mf} = minimum fluidizing velocity (m/s)
ω = mass based conversion of the oxygen carrier
$\omega_{f,red}$ = final conversion of the oxygen carrier in the previous reduction
x_i = molar fraction of the gas species i
γ_o = oxygen yield

REFERENCES

(1) Richter, H.; Knoche, K. Reversibility of combustion processes. *ACS Symp. Ser.* **1983**, *235*, 71.

(2) Ishida, M.; Jin, H. A novel chemical looping combustor without NO_x formation. *Ind. Eng. Chem. Res.* **1996**, *35*, 2469.

(3) Ishida, M.; Jin, H. CO_2 recovery in a power plant with chemical looping combustion. *Energy Convers. Manage.* **1997**, *38*, S187.

(4) Lyngfelt, A.; Leckner, B.; Mattisson, T. A fluidized-bed combustion process with inherent CO_2 separation; Application of chemical-looping combustion. *Chem. Eng. Sci.* **2001**, *56*, 3101.

(5) Lyngfelt, A.; Thunman, H. Construction and 100 h of operational experience of a 10 kW chemical-looping combustor. *The CO_2 Capture and Storage Project (CCP) for Carbon Dioxide Storage in Deep Geologic Formations For Climate Change Mitigation*; Elsevier Science: London, 2005; Vol. *1*.

(6) Markström, P.; Lyngfelt, A. Designing and operating a cold-flow model of a 100 kW chemical-looping combustor. *Powder Technol.* **2012**, *222*, 182.

(7) Kolbitsch, P.; Bolhar-Nordenkampf, J.; Proll, T.; Hofbauer, H. Operating experience with chemical looping combustion in a 120 kW dual circulating fluidized bed (DCFB) unit. *Int. J. Greenhouse Gas Control* **2010**, *4*, 180.

(8) Galloy, A.; Strohle, J.; Epple, B. Design and operation of a 1 MWth carbonate and chemical looping CCS test rig. *VGB PowerTech.* **2011**, *91*, 64.

(9) Andrus, H.; Chui, J.; Thibeault, P.; Edberg, C.; Turek, D.; Kenney, J.; Abdulally, I.; Chapman, P.; Kang, S.; Lani, B. Alstom's limestone-based chemical looping process. 2nd International Conference on Chemical Looping, September 26−28, Darmstadt, Germany; 2012.

(10) CCBJ Weekly News July 20, 2012. http://www.climatechangebusiness.com/Climate_Change_Weekly_News_July_20_2012 (accessed July 2012).

(11) Xu, L.; Wang, J.; Li, Z.; Cai, N. Experimental study of cement-supported CuO oxygen carriers in chemical looping with oxygen uncoupling (CLOU). *Energy Fuels* **2013**, *27*, 1522.

(12) Adanez, J.; Abad, A.; Garcia-Labiano, F.; Gayán, P.; de Diego, L. F. Progress in chemical-looping combustion and reforming technologies. *Prog. Energy Combust. Sci.* **2012**, *38*, 215.

(13) Lyngfelt, A. Chemical-looping combustion of solid fuels—Status of development. 2nd International Conference on Chemical Looping, September 26−28, Darmstadt, Germany; 2012.

(14) Shulman, A.; Linderholm, C.; Mattisson, T.; Lyngfelt, A. High reactivity and mechanical durability of $NiO/NiAl_2O_4$ and $NiO/NiAl_2O_4/MgAl_2O_4$ oxygen carrier particles used for more than 1000 h in a 10 kW CLC reactor. *Ind. Eng. Chem. Res.* **2009**, *48*, 7400.

(15) Kolbitsch, P.; Bolhar-Nordenkampf, J.; Proll, T.; Hofbauer, H. Comparison of two Ni-based oxygen carriers for chemical looping combustion of natural gas in 140 kW continuous looping operation. *Ind. Eng. Chem. Res.* **2009**, *48*, 5542.
(16) de Diego, L. F.; García-Labiano, F.; Gayán, P.; Celaya, J.; Palacios, J. M.; Adanez, J. Operation of a 10 kWth chemical-looping combustor during 200 h with a CuO-Al_2O_3 oxygen carrier. *Fuel* **2007**, *86*, 1036.
(17) Gu, H.; Shen, L.; Xiao, J.; Zhang, S.; Song, T. Chemical looping combustion of biomass/coal with natural iron ore as oxygen carrier in a continuous reactor. *Energy Fuels* **2011**, *25*, 446.
(18) Xiao, R.; Song, Q.; Zhang, S.; Zheng, W.; Yang, Y. Pressurized chemical-looping combustion of Chinese bituminous coal: cyclic performance and characterization of iron ore-based oxygen carrier. *Energy Fuels* **2010**, *24*, 1449.
(19) Xiao, R.; Song, Q.; Song, M.; Lu, Z.; Zhang, S.; Shen, L. Pressurized chemical-looping combustion of coal with an iron ore-based oxygen carrier. *Combust. Flame* **2010**, *157*, 1140.
(20) Leion, H.; Jerndal, E.; Steenari, B. M.; Hermansson, S.; Israelsson, M.; Jansson, E.; Johnsson, M.; Thunberg, R.; Vadenbo, A.; Mattisson, T.; Lyngfelt, A. Solid fuels in chemical-looping combustion using oxide scale and unprocessed iron ore as oxygen carriers. *Fuel* **2009**, *88*, 1945.
(21) Linderholm, C.; Lyngfelt, A.; Cuadrat, A.; Jerndal, E. Chemical-looping combustion of solid fuels—Operation in a 10 kW unit with two fuels, above-bed and in-bed fuel feed and two oxygen carriers, manganese ore and ilmenite. *Fuel* **2012**, *102*, 808.
(22) Wen, Y.; Li, Z.; Xu, L.; Cai, N. Experimental study of natural Cu ore particles as oxygen carriers in chemical looping with oxygen uncoupling (CLOU). *Energy Fuels* **2012**, *26*, 3919.
(23) Leion, H. Use of ores and industrial products as oxygen carriers in chemical-looping combustion. *Energy Fuels* **2009**, *23*, 2307.
(24) Mendiara, T.; Abad, A.; de Diego, L. F.; García-Labiano, F.; Gayán, P.; Adanez, J. Use of an Fe-based residue from alumina production as an oxygen carrier in chemical-looping combustion. *Energy Fuels* **2012**, *26*, 1420.
(25) Adanez, J.; Cuadrat, A.; Abad, A.; Gayán, P.; de Diego, L. F.; García-Labiano, F. Ilmenite activation during consecutive redox cycles in chemical-looping combustion. *Energy Fuels* **2010**, *24*, 1402.
(26) Abad, A.; Adanez, J.; Cuadrat, A.; García-Labiano, F.; Gayán, P.; de Diego, L. F. Kinetics of redox reactions of ilmenite for chemical-looping combustion. *Chem. Eng. Sci.* **2011**, *66*, 689.
(27) Leion, H.; Lyngfelt, A.; Johansson, M.; Jerndal, E.; Mattisson, T. The use of ilmenite as an oxygen carrier in chemical-looping combustion. *Chem. Eng. Res. Des.* **2008**, *86*, 1017.
(28) Leion, H.; Mattisson, T.; Lyngfelt, A. Solid fuels in chemical-looping combustion. *Int. J. Greenhouse Gas Control* **2008**, *2*, 180.
(29) Azis, M. M.; Jerndal, E.; Leion, H.; Mattisson, T.; Lyngfelt, A. On the evaluation of synthetic and natural ilmenite using syngas as fuel in chemical-looping combustion (CLC). *Chem. Eng. Res. Des.* **2010**, *88*, 1505.
(30) Cuadrat, A.; Abad, A.; Adánez, J.; de Diego, L. F.; García-Labiano, F.; Gayán, P. Behavior of ilmenite as oxygen carrier in chemical-looping combustion. *Fuel Process. Technol.* **2012**, *94*, 101.
(31) Schwebel, G. L.; Leion, H.; Krumm, W. Comparison of natural ilmenites as oxygen carriers in chemical-looping combustion and influence of water gas shift reaction on gas composition. *Chem. Eng. Res. Des.* **2012**, *90*, 1351.
(32) Cuadrat, A.; Abad, A.; García-Labiano, F.; Gayán, P.; de Diego, L. F.; Adánez, J. The use of ilmenite as oxygen-carrier in a 500 Wth chemical-looping coal combustion unit. *Int. J. Greenhouse Gas Control* **2011**, *5*, 1630.
(33) Berguerand, N.; Lyngfelt, A. Design and operation of a 10 kWth chemical-looping combustor for solid fuels-testing with South African coal. *Fuel* **2008**, *87*, 2713.
(34) Berguerand, N.; Lyngfelt, A. Batch testing of solid fuels with ilmenite in a 10 kWth chemical-looping combustor. *Fuel* **2010**, *89*, 1749.
(35) Bidwe, A. R.; Mayer, F.; Hawthorne, C.; Charitos, A.; Schuster, A.; Scheffknecht, G. Use of ilmenite as an oxygen carrier in chemical looping combustion—Batch and continuous dual fluidized bed investigation. *Energy Procedia* **2011**, *4*, 433.
(36) Thon, A.; Kramp, M.; Hartge, E. U.; Heinrich, S.; Werther, J. Operational experience with a fluidized bed system for chemical looping combustion of solid fuels. In 2nd International Conference on Chemical Looping, September 26–28, Darmstadt, Germany; 2012.
(37) Markström, P.; Lyngfelt, A.; Linderholm, C. Chemical looping combustion in a 100 kW unit for solid fuels. In 21st International Conference on Fluidized Bed Combustion, June 3–6, Naples, Italy; 2012.
(38) Mendiara, T.; Pérez, R.; Abad, A.; de Diego, L. F.; García-Labiano, F.; Gayan, P.; Adanez, J. Low-cost Fe-based oxygen carrier materials for the iG-CLC process with coal. 1. *Ind. Eng. Chem. Res.* **2012**, *51*, 16216.
(39) Abad, A. Low-cost Fe-based oxygen carrier materials for the iG-CLC process with coal. 2. *Ind. Eng. Chem. Res.* **2012**, *51*, 16230.
(40) Bao, J.; Li, Z.; Sun, H.; Cai, N. Experiment and rate equation modeling of Fe oxidation kinetics in chemical looping combustion. *Combust. Flame* **2013**, *160*, 808.
(41) Paneth, H. R. The mechanism of self-diffusion in alkali metals. *Phys. Rev.* **1950**, *80*, 708.
(42) Johansson, H.; Byegard, J.; Skarnemark, G. Matrix diffusion of some alkali- and alkaline earth-metals in granitic rock. *Sci. Basis Nuclear Waste Manage. XX Symp.* **1997**, 871.
(43) Yang, J.; Cai, N.; Li, Z. Hydrogen production from the steam-iron process with direct reduction of iron oxide by chemical looping combustion of coal char. *Energy Fuels* **2008**, *22*, 2570.
(44) Wen, C. Y.; Yu, Y. H. A generalized method for predicting the minimum fluidization velocity. *AlChE J.* **1966**, *12*, 610.
(45) Bao, J.; Liu, W.; Cleeton, J. P. E.; Scott, S. A.; Dennis, J. S.; Li, Z.; Cai, N. Interaction between Fe-based oxygen carriers and *n*-heptane during chemical looping combustion. *Proc. Combust. Inst.* **2013**, *34*, 2839.
(46) Yin, Y.; Rioux, R. M.; Erdonmez, C. K.; Hughes, S.; Somorjai, G. A.; Alivisatos, A. P. Formation of hollow nanocrystals through the nanoscale Kirkendall effect. *Science* **2004**, *304*, 711.
(47) Fan, H. J.; Gçsele, U.; Zacharias, M. Formation of nanotubes and hollow nanoparticles based on Kirkendall and diffusion processes: A review. *Small* **2007**, *3*, 1660.
(48) Rao, D. B.; Rigaud, M. Kinetics of the oxidation of ilmenite. *Oxid. Met.* **1975**, *9*, 99.
(49) Muhler, M.; Schlogl, R.; Reller, A.; Ertl, G. The nature of the active phase of the Fe/K-catalyst for dehydrogenation of ethylbenzene. *Catal. Lett.* **1989**, *2*, 201.
(50) Tran, K. Q.; Iisa, K.; Hagström, M.; Steenari, B. M.; Lindqvist, O.; Pettersson, J. B. C. On the application of surface ionization detector for the study of alkali capture by kaolin in a fixed bed reactor. *Fuel* **2004**, *83*, 807.
(51) Sun, D.; Sung, W.; Chen, R. The release behavior of potassium and sodium in the biomass high-temperature entrained-flow gasification. *Appl. Mech. Mater.* **2011**, *71–78*, 2434.